Mapana – Journal of Sciences
2023, Vol. 22, No. 1, 147-175
ISSN 0975-3303 | https://doi.org/10.12723/mjs.64.8

CT-DNA Interaction, Fluorescence Binding and Microbial Activities of Schiff Base Ligand Metal Complexes Derived from 4-Bromobenzaldehyde and 2-Amino-6-Methylbenzothiazole

G. Senthamilselvan*†, A. Palanimurugan†, B. Sithi Asma†, A. Cyril†

Abstract

Bidentate ligand (L) was synthesized by knoevenagel reaction using 4-bromobenzaldehyde and 2-amino-6-methylbenzothiazole. The ligand has been confirmed from the analytical technique such as UV-Vis, FTIR, NMR, Mass and EPR spectral. The synthesized metal complexes were characterized from the spectra and physico-chemical techniques. These studies showed that the stoichiometric composition of ML_2 type complexes. Absorption study implies that the compounds possess the octahedral geometry and their chelates are electrolytic and monomeric in nature. Absorption and gel electrophoresis experiments set up accepted the effective interaction with CT-DNA molecules. It was extended to Fluorescence emission study of binding. The anti-bacterial and anti-fungi studies were carried out by disc diffusion method. From the MIC values, metal complexes were controlling larger than Schiff base.

* Department of Industrial Chemistry, Alagappa University, Karaikudi, Tamil Nadu, India; genishiyapalani@gmail.com

† Post Graduate and Research Department of Chemistry, Raja Doraisingam Government Arts College, Sivagangai - 630 561, Tamil Nadu, India; cyrilchemistry@gmail.com

Keywords: 2-amino-6-methylbenzothiazole based ligand; metal complexes; CT-DNA binding; Fluroscence; anti-microbial study

1. Introduction

In present days, interesting study has rewarded for Schiff base transition metal compounds. The synthetic and structural characterization of transition metal complexes is essential in the developments of new synthetic models of some enzymes. In coordination chemistry the metal ions coordinate with other ligands to form covalent bonds. Schiff bases (SBs) size can enhance by one unit derived after have >C=N- bond. In that an aryl or alkyl group linked with nitrogen atom except for hydrogen [(1)]. The knoevenagal reaction of primary amines with aldehyde or ketones, yield the Schiff bases and they were discovered in the year of 1864 by a German chemist named Hugo Schiff. It has azomethine (>C=N) group and $R_1R_2C=NR_3$ structure where R_1, R_2 and R_3 may be aryl, alkyl, cycloalkyl or heterocyclic groups. The nature of bonding in ligand depends on the coordinate sites such as N, S, and O, electro negativities. Schiff base active ligands presence of electro negativity atom of nitrogen, azomethine group (>C=N), electron pair on the nitrogen and metal activities regulated for variety of biological and catalytic conversional studies [(2)].

From three decades, great attention was rewarded to the transition metal compounds of the imines due to their stability and vast applications including biological fields. Schiff base complexes have also used and widely studied in, antifungal, antibacterial, anticancer, antiviral and herbicidal studies. It served as biologically models for active species and finding new application in biomimetic activities. The biomolecules bonded to the metal ions could enhance their bioactivities. Some molecules do not function normally without their implausible in living organisms. These metals from alkali metals and transition elements are called as 'metals of life'. The presence of trace quantities of these metals may play crucial roles at the molecular level in all livings. Particularly the transition metal's roles are well known in regulation of growth and metabolism of living system [(3)]. Hence, the synthetic coordination compounds of these metal complexes have urged significantly in modern bioinorganic [(4-7)].

The complexes of DNA-metal is interesting studies and passionate research. The non-covalent binding may be through mainly electrostatic, intercalation, and groove [8–9]. The geometry of metal chelates and interactions of DNA are interconnected. Transformations to DNA and drug molecules are required as a result of binding interactions to allow complex formation. In the majority of studies, modifications of DNA led to alter the thermodynamic stability and the functional characteristics. Metal ions, which are crucial components in natural enzymatic action and are used in the hydrolysis reactions of nucleic acids, are brought into the design of synthetic controlled end nucleases by chemists. While performing functions like acidity and polarizing the phosphorous oxygen bond to facilitate bond breakage, metal complexes can be very effective in promoting the hydrolysis of phosphodiester. DNA fragments produced by metal complexes cleaving DNA under hydrolytic conditions may be controlled similarly to restriction enzymes [10–14]. The majority of earlier reports on DNA cleavage activity are restricted to oxidative cleavage, which for its primary applications necessitates the inclusion of an external property to cleavage and restricted initiation. The separation of heterolytic agents does not remove crucial co-reactants from the reaction.

The imine compounds and their chelates have been shown to be toxic to human and rodent cell lines in tissue culture as well as to have antimicrobial activity against microbes. Good antibacterial, fungicidal, insecticidal, and herbicidal activities could be found in the majority of organic ligands. According to a literature review, metal complexes with biologically active metal compounds are frequently formed, which changes the activity. Metal chelates were essential in the development of biosystems where enzymatic activity is thought to be supported by metals. The metal ions, which are present in enzymes, function as cofactors for their enzymatic properties. The heterocyclic compounds with N, O, and S atoms form cyclic rings without strain and produce 1:2 chelates with transition metals, which showed significant antibacterial properties [15-19].

The diffusion, cell membrane permeability and the spatial arrangement favor the passage of lipid-soluble materials that could control antimicrobial effects by enhancing liposolubility. The

increased lipid solubility of the metal chelates made it easier for them to penetrate through microorganisms, which may have led to increase the cell permeability. The literature mentioned above highlights the significance of biological screening studies using metal ions, heterocyclic compounds, etc., which heavily depend on the type of microorganism.

The 4-bromo benzaldehyde has two coordinating sites and can be converted into desired derivatives by condensing with the right reagents. In this study, a imine based ligand was synthesized using condensation between 4-Bromobenzaldehyde and 2-amino 6-methylbenzothiazole. The structural characterizations of produced metal chelates were examined using various sophisticated analytical instruments, including FT-IR, ESR, NMR, UV-Visible, ESI-MS, and molecular susceptibility. The bioactivity investigations of metal complexes were conducted into the bacteria and fungi. This work also deals with the nuclease activity of active metal chelates that binds DNA through redox chemistry.

2. Experimental

2. 1 Materials

2-amino-6-methylbenzothiazole ($C_8H_8N_2S$; E. Merck), 4-bromobenzaldehyde (C_7H_5BrO; E.Merck), Copper(II) chloride dihydrate ($CuCl_2.\ 2H_2O$; SD Fine) Anhydrous zinc (II) chloride ($ZnCl_2$; SD Fine), Nickel chloride ($NiCl_2$; SD Fine), Cobalt chloride ($CoCl_2$;SD Fine) and methanol were purchased and used for synthesis and characterizations.

2. 2 Micro-Analytical Characterization Methods

2. 2.1 Instrumentation

Elemental Vario ELIII CarloErba1108 (SAIF, Lucknow) was used to record the elemental analysis of imines and metal chelates, including carbon, hydrogen, and nitrogen atoms. In the microanalysis, a sample containing a tiny capsule and weighing about 10 mg was injected into the apparatus to determine the computerized elemental percentage (the data are shown in **Table 1**). EDTA was used for calibrating the instrument. Shimadzu FT-IR Affinity-1 spectrophotometer was used to record the IR spectra of

imines and metal chelates as potassium bromide discs in the 400–4000 cm^{-1} range. The Shimadzu UV-1800 spectrometer was used to record the optical absorption property of the imine and its metal chelates in the 200–1100 nm wavelength range. 400 MHz NMR studies of the samples recorded over Bruker Avance DRX400FT-NMR spectrometer recorded at CECRI, Karaikudi using tetramethyl silane. The ESI-MS (SAIF, Lucknow) of the complexes was captured using the JEOLSX102/DA-6000 spectrometer system used by Ar/Xe (6kV,10mA). At room temperature (RT), m-nitro benzyl alcohol (NBA) matrixes were used to record the spectral evidences at an accelerating voltage of 10 kV. On a Varian E-112 spectrometer (SAIF, Mumbai) with 100 kHz, the EPR spectra of metal chelates were captured in the X-band regions.

2.2.2 Metal Determination

Through the fusion of their oxides with analytic ammonium oxalate, the metals were analyzed and gravimetrically estimated. In a test, 0.3g of dried samples was precisely weighed in a silica crucible. Using a Bunsen burner, ammonium oxalate (AR) in 3 parts by weight of complexes was incinerated about 3 hours. The resultant compound was weighed after cooling in a desiccator. This procedure was continued until the mass of oxide became same and then metal content was estimated quantitatively [20].

2. 2.3 Determination of Chloride

Chloride present in the complexes was determined gravimetrically by treating with silver nitrate and precipitated as silver chloride [21].

2.2.4 Determination of Molar Conductance (Λ_m)

Measurements of molar conductance of the chelates in solution were designed primarily to determine the ionic formulation of the metal complexes, or whether the metal salts' anions retain inside or outside the central metal atom's coordination sites. Using the appropriate solvent, the conductivities of the complexes were examined in a 601 digital molar conductivity instrument. All adjusted measurements were used to calculate the pure solvent conductance by deducting the conductance of the relevant solution. The degree of dissociation, mobility of metal, the temperature, and

the number of ions in the available solution all affect molar conductance in a given solvent. The conductivity of the complexes was determined using the formula:

$$\Lambda_m = (1000 \times \text{Cell constant} \times \text{conductance}) / \text{Concentration}$$

The results are compared to industry standards using research literature to determine the complexes' nature, including whether they are electrolytes or non-electrolytes [22].

2. 2.5 Magnetic Susceptibility and Magnetic Moments

Using a Gouy type magnetic balance the magnetic susceptibility measurements were made for the solid copper (II) sample. We measured the weight changes using a Mettler electrochemical balance. A magnetic field produced by an electromagnet had strength of about 8000 Gauss. A string without twists was used to suspend the Gouy tube. The empty tube was held in place by two magnetic poles. The bottom of tube was half way between the poles and at inter pole axis. The weight of tube was taken in presence/absence of magnetic field. The tube was then filled with finely ground complex in order to minimize the error and the above procedure was repeated.

The paramagnetic properties of the metal complexes were designed elucidative determination from its extent the gain in weight experienced by the sample under the applied magnetic field using the following relation:

$$\chi p = \alpha + \beta F' / W$$

Where, χp = paramagnetic susceptibility; α = 0.029 x volume correction (air correction), β = Tube calibration constant; W = Substance Weight in gram (G), F'= change in weight of the sample under applied field with necessary diamagnetic correlation Gouy tube. The tube calibration constant was determined using copper sulphate penta hydrate as calibrate. Molar susceptibility is the product of molecular weight of the samples and paramagnetic susceptibility. Diamagnetic correlations using Pascal's constants applied by added the diamagnetic contributions of many atoms and its structural units [23]. The given corrected magnetic susceptibility, where χm is used to obtained the effective magnetic moment from Lang ham expressions.

The magnetic moment values (μ_{eff}) of the metal chelates can be calculated as below,

μ_{eff} = 2.84 [χmT]1/2 B.M.

Where, χm = Molar susceptibility (B.M), T = Absolute temperature (K)

This determines the number of unpaired electrons 'n' and its availability possessed by the metal chelates. The unpaired electrons would be interacting with the valence band of metal complexes [24]. The given data helped to find out the complexes whether high or low spin states.

2.3 Preparation Tris-HCl Buffer

Accurately weighed amounts of Tris-HCl (5 mM) and NaCl (50 mM) were dissolved with double-distilled water (DDW) in a standard measuring flask (SMF) to a volume of 250 mL. By adding 1 mM NaOH, the pH was brought down to 7.2 using a pH meter (Roy Instruments, RI501 model).

2.4 Metal-DNA Interaction Studies

The optical absorption technique was used to carry out the CT-DNA binding studies. In Tris-HCl buffer (pH =7.2) with 50 mM NaCl the relativity of binding modes was extensively studied. The ratio UV ranges at 260/280 nm were discovered using the provided CT-DNA solution. The measured values, which are DNA molecules sufficiently free of protein, range from 1.8 to 1.9. When used for their preparation after 72 hours (3 days), the stock solution was kept at the same pH as the Tris-Hcl buffer and was stored at 4 ^{o}C. The optical absorption intensity at 260 nm was used to calculate the molar extinction coefficient, which was found to be 6600 $M^{-1}cm^{-1}$.

2.5 Electronic Spectra

In Tris-HCl buffer (pH =7.2) with 50 mM NaCl, the absorption of metal chelates were examined with and without DNA. By adding DNA solution to metal complexes as needed, intercalation modes were observed from the absorption data. The same titration was repeated in order to determine their actual

saturation. The DNA]/(ε_a-ε_f) *vs.* [DNA] plot from (1) is used to determine the binding constant (K_b).

$$[DNA]/ (\varepsilon_a-\varepsilon_f) = [DNA]/ (\varepsilon_b-\varepsilon_f) + 1/[K_b(\varepsilon_b-\varepsilon_f)] \text{ ------(1)}$$

Where, [DNA]- DNA concentration; Extinction coefficient A_{obs}/[complex], free complex, the complex bound are ε_a, ε_f and ε_b respectively.

$$E°_b - E°_f = 0.0591 \log (K_R/ K_O) \text{ ------ (2)}$$

Where, binding constants K_R and K_o are the reduced and oxidized species to CT-DNA, E°b and E°f are bound and free chelates formal potentials [26]. The dispersion of the metal chelates in to CT-DNA may decrease the voltammetry currents upon interaction with CT-DNA. This demonstrated how strongly the complex's binding affinity to CT-DNA molecules.

2.6 Viscosity Study

Using an Ostwald viscometer, the viscosity of CT-DNA with metal complexes was observed. Complexes are concentrated at a fixed volume of CT-DNA solution. It takes an average digital stopwatch three attempts to check and measure fluidity. The lengthening of DNA base pairs causes a classical intercalation EB to exhibit increases in relative viscosity. However, if the mode of decreased viscosity values with non-intercalation (or) partial interactions made the DNA helix bend, the length of DNA would continuously decrease. The calculations were also made of CT DNA's viscosity in the presence (η) and absence (η_0) of complexes [27]. After all measurement plotting the ratio of $(\eta/ \eta_0)^{1/3}$ against 1/R reveals that R=([complex]/[DNA]) represents the relative time of viscosity.

2.7 Antimicrobial Activities

2.7.1 Antibacterial Studies

The standard nutritional agar is the medium used to test the activities of particular microorganisms (antibacterial agents). About 3g of beef extract, 5g of peptone and yeast extracts, and 5g of NaCl were dissolved in 1L of double-distilled water (DDW) in a clean conical flask to create the nutrient agar medium. After maintaining pH=7, the items are boiled and autoclave sterilized for 30 minutes at

120 ^{o}C. After sterilization, 20 mL of media was added to the Petri plates and left for some time to solidify. Then, using sterile swabs, it was inoculated with the proper microorganisms. By dissolving the metal complexes in an appropriate solvent medium, the stock solutions were created. By using a micropipette to fill test solutions into a disc that was 1 mm thick and 5 mm in diameter, the antibacterial properties of metal complexes were assessed against the pathogenic bacteria [28]. The discs were then closely incubated at 37 ^{o}C for about 24 hours. The inoculated bacteria's growth was impacted by the diffusion of the test solution. It was observed and measured as the inhibition zone on the plate changed over time.

2.7.2 Antifungal Studies

Standard potato dextrose agars were used in the studies as the testing medium to determine whether microorganisms had any antibacterial activity. In order to create the dextrose-agar medium, agar (20 g), potato extract (200 g), and dextrose (20 g) were dispersed in 1 L of DDW. Using an autoclave machine, this is thoroughly sterilized for 30 minutes at 120 ^{o}C and 15 lbs of pressure. Repeating the experimental setup and finally selecting the appropriate microorganisms involved the same process. The antifungal properties of complexes have been evaluated for biological studies using the same metrics as mentioned above.

2.7.3 Determination of MIC

The Schiff base metal complexes have chosen to determine the MIC values due to their potent antibacterial and antifungal properties. The lower concentration of antimicrobial compounds, as determined by MIC values, will prevent the growth of particular microorganisms during incubation periods. To monitor the effectiveness of new antimicrobial agents and their standards, microorganism reduction is necessary.

2. 8 Preparation of Ligand (L)

The **Schemes 1** illustrate the schematic synthesis of Schiff base. By dissolving equimolar amount of 2-amino-6-methylbenzothiazole and 4-bromobenzaldehyde in Methanol, a ligand was created. The mixture was then stirred for approximately 5 hours. After being separated by filtration, cleaned with redistilled

water, recrystallized from ethanol, and dried, a yellow-colored Schiff base condensate was produced. Lastly, it was kept dry in a vacuum desiccator.

[$C_{15}H_{11}BrN_2S$](L): Yield (%): 74, M.Wt: 331.23, Anal. Calc. (%): C, 53.39; H, 3.35; N, 8.46; S, 9.68 obtained (%): C, 53.25; H, 3.27; N, 8.12; S, 9.27. ^{1}H-NMR (δ/ppm): 7.30–8.00 (Ph–H), 8.36 (CH═N), FTIR (ν/cm^{-1}): 1643 ν[(CH═N) (azomethine)]; UV–Vis (DMF, λ_{max}/cm^{-1}): 36,764 and 30,120.

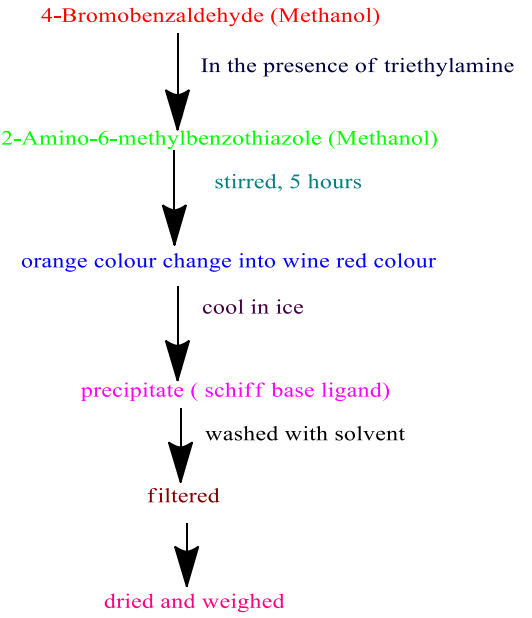

Scheme 1. Flow chart for the synthesis Schiff base Ligand

2.9 Preparation of Metal Complexes

The Schiff bases (0.512g, 2 mmol) in methanolic solution (25 ml) were combined with $CoCl_2.6H_2O$ (0.237g, 1 mmol), $NiCl_2.6H_2O$ (0.237g, 1 mmol), $CuCl_2.2H_2O$ (0.170g, mmol), and $ZnCl_2$ (0.136 g, 1 mmol) separately and refluxed for about 3 hours (**Scheme 2**). The complexes were separated, washed, vacuumed dried over fused $CaCl_2$.

[$CuC_{32}H_{28}Br_2N_4S_2Cl_2$](1): Yield (%): 72, M.Wt: 826.98,Anal. Calc. (%): Cu, 7.68; C, 45.48; H, 3.42; N, 6.77; S, 9.68; Cl, 8.57 Found (%): Cu,

7.52; C, 45.39; H, 3.56; N, 6.53; S, 9.71; Cl, 8.46. FTIR (ν/cm^{-1}): 1637 ν[(CH=N-)(azomethine)], 530 ν(Cu–O), 428 ν(Cu-N); UV-Visible (λ_{max}/cm^{-1}): 36,363, 30,303 and 18,796; molar conductance: 14.3 cm^2 ohm^{-1} mol^{-1}; μ_{eff} : 1.95 (B.M.)

[ZnC$_{32}$H$_{28}$Br$_2$N$_4$S$_2$Cl$_2$](2): Yield (%): 68, M.Wt: 828.8 , Anal. Calc. (%): Zn, 7.89; C, 46.37; H, 3.41; N, 6.76; S, 7.74; Cl, 8.56. Found (%): Zn, 6.72; C, 46.23; H, 3.35; N, 6.64; S, 7.67; Cl, 8.12. ^{1}H NMR (δ/ppm): 6.9-8.1 (Ar–H), 8.72 (CH=N-), FTIR (ν/cm^{-1}): 1641 ν[(CH=N)(azomethine)], 528 ν(Zn-Cl), 452 ν(Zn-N); UV-Visible (λ_{max}/cm^{-1}): 35,460 and 29,940; molar conductance: 19.7 cm^2 ohm^{-1} mol^{-1}; μeff : diamagnetic.

[NiC$_{32}$H$_{28}$Br$_2$N$_4$S$_2$Cl$_2$](3): Yield (%): 65, M.Wt: 822.1,Anal. Calc. (%): Ni, 7.31; C, 46.75; H, 3.43; N, 6.72; S, 7.63; Cl, 8.40 Found (%): Ni, 7.11; C, 46.67; H, 3.32; N, 6.74; S, 7.53; Cl, 8.38. FTIR (ν/cm^{-1}): 1637 ν[(CH=N-) (azomethine)], 530 ν(Ni-O), 428 ν(Ni-N); UV-Visible (λ_{max}/cm^{-1}): 36,363, 30,303 and 18,796; molar conductance : 14.3 cm^2 ohm^{-1} mol^{-1}; μ_{eff} : 1.95. (B.M.)

[CoC$_{32}$H$_{28}$Br$_2$N$_4$S$_2$Cl$_2$](4): Yield (%): 69, M.Wt: 822 , Anal. Calc. (%): Co, 7.17; C, 46.74; H, 3.43; N, 6.81; S, 7.80; Cl, 8.62 Found (%): Co, 6,89; C, 46.39; H, 3.36; N, 6.53; S, 7.57; Cl, 8.46. FTIR (ν/cm^{-1}): 1637 ν[(CH=N-)(azomethine)], 530 ν(Co-O), 428 ν(Co-N); UV-Visible (λ_{max}/cm^{-1}): 36,363, 30,303 and 18,796; molar conductance: 14.3 cm^2 ohm^{-1} mol^{-1}; μ_{eff} : 1.95. (B.M.)

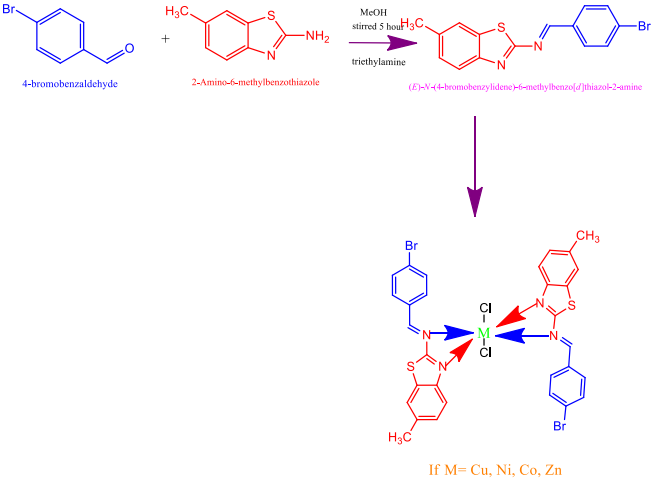

Scheme 2. Schematic representation for the preparation of metal complexes

3. Results and Discussions

The ligand and metal chelates were synthesized and it has been discovered that they are air stable. DMSO is only solvent to dissolve the metal chelates, while the ligand soluble in $CHCl_3$, DMSO, and DMF. Utilizing spectral and analytical methods, ligand and metal chelates were identified. The observed molar conductance and magnetic susceptibility of metal complexes were shown below. The analytical information for the metal complexes is in accordance with the general formula ML_2, where M is equal to Cu(II), Co(II), Ni(II), and Zn(II). When the central metal ion is surrounded by an octahedral structure, the magnetic susceptibility measurements of the metal chelates were accurate. The chelate's high conductance values confirm their conductivity and electrolytic in nature.

3.1 FT-IR Spectra

FTIR spectra provide useful information about the same site of ligands. To confirm the effectiveness of changes that have occurred during complexation, the spectra of metal chelates were compared with spectra of ligand. Certain peaks are seen frequently in the relative IR spectra of the ligand and their metal chelates. In these spectra some significant peaks that were obtained and are either shifted or newly appeared. As shown in **Figure 1**, the ligand's' both thiazole ring and azomethine group were vibrating in the region of 1653 cm^{-1}. After complexation, these values (thiazole ring) were elevated and (azomethine group) shifted to lower frequencies.

The bands in region 761-725 cm^{-1} that remain in the same location after complexation and in free ligands indicate that the sulfur atom in the thiazole group does not coordinate with metal in complexes [29]. The spectra of metal chelates appeared new in weak range 420-435 cm^{-1}, and a band due to M-Cl appeared in 400 cm^{-1} range.

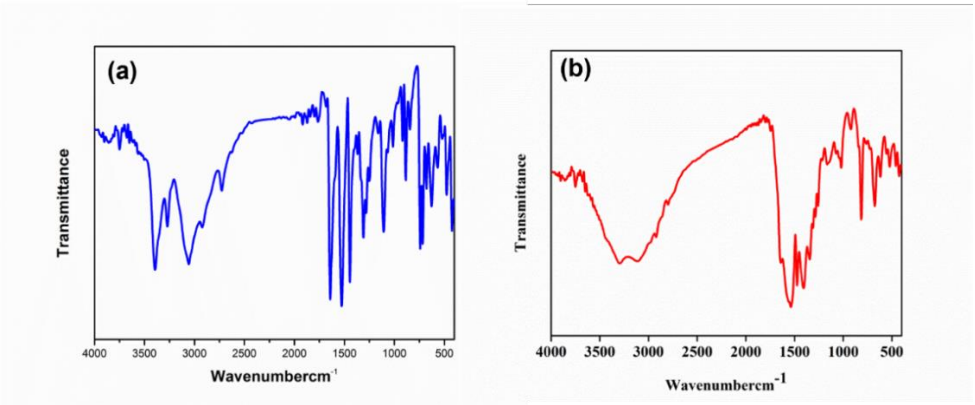

Figure 1. FTIR spectra of (a) Ligand and (b) CuL_2Cl_2 chelate

3.2 UV-V is Spectroscopy

The arrangement of ligands in metal chelates may be quickly and accurately revealed by the electronic spectra. **Figure 2** displays the UV-Vis spectra of ligand and metal chelates. A absorption band at a wavelength of 27778 cm^{-1} was attributed to the n → π* transition in ligand. The d-d transition, also known as the $^1A_{1g} \rightarrow {}^1B_{1g}$ transition in copper (II) complex, is visible at 14705 cm^{-1}. Its magnetic moment value (1.86 B.M) demonstrates that the copper (II) complexes exist in distorted octahedral geometry. The measured cobalt (II) magnetic moment value (4.79 B.M) is greater than the measured spin-only moment value (3.87 B.M). This is because of their unpaired electrons, which are applicable to high spin octahedral Cobalt (II) complexes and show bands at 13793 cm^{-1} that may have the presence of the $^2E_g \rightarrow {}^2T_{2g}$ transition, respectively. The magnetic moment for nickel (II) complexes is 3.43 B.M., and the spectra of these complexes exhibit bands at 14084 cm^{-1}, which may indicate the presence of the $^1A_{1g} \rightarrow {}^1A_{2g}$ transition, suggesting an octahedral configuration. The magnetic moments and the various transition data were displayed in **Table 2**.

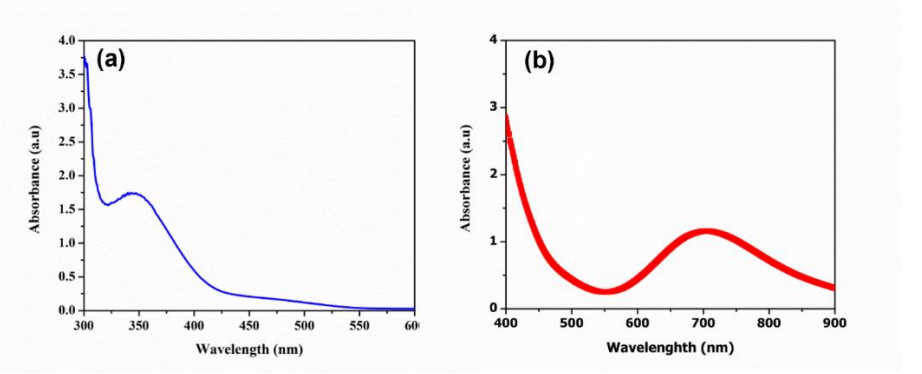

Figure 2. Visible spectra of (a) Schiff base and (b) CuL_2Cl_2 chelate

Table 1 Physical and elemental analysis data of Ligand and transition metal chelates

Compound	Found (Calc)%					Formula weight	Molar conductance $\Omega^{-1}cm^{-2}$ mol^{-1}	μ_{eff} (B.M)
	M	C	H	N	S			
Ligand	-	54.39 (53.25)	3.35 (3.27)	8.46 (8.12)	9.68 (9.27)	329	-	-
$[CuL_2Cl_2]$	7.68 (7.52)	46.48 (46.39)	3.41 (3.56)	6.77 (6.53)	9.68 (9.7)	826	14.1	1.93
$[NiL_2Cl_2]$	7.41 (7.11)	46.75 (46.67)	3.43 (3.32)	6.81 (6.74)	7.80 (7.53)	822	16.2	3.56
$[CoL_2Cl2]$	7.17 (6.89)	46.74 (46.39)	3.43 (3.36)	6.81 (6.53)	7.80 (7.57)	821	17.9	4.31
$[ZnL_2Cl2]$	7.89 (6.72)	46.37 (46.32)	3.41 (3.35)	6.76 (6.64)	7.74 (7.67)	828	19.3	Dia

Table 2. The various transition data and the values of magnetic moment

Compound	π-π*	n- π*	d-d	μ_{eff} (B.M)
Ligand	258	305	-	-
Cu-L_2	281	386	718	1.93
Co-L_2	265	398	693	4.31
Ni-L_2	267	361	623	-
Zn-L_2	279	425	710,722	-

3.3 NMR Spectroscopy Studies

In DMSO-d6, the ^{1}H-NMR spectra of ligand (L) and the CuL_2 metal chelate were captured using TMS (**Figures 3a)** and ^{13}C-NMR (**Figures 3a).** The aromatic protons can be seen in multiplet at 6.94–7.98 ppm in ^{1}H NMR spectrum of the ligand (L). It also exhibits a singlet at 9.70 ppm caused by the proton in the azomethine (-CH=N) group and 3.86 ppm caused by the (Ph-Br) group. Upon coordination of ligand with a metal ion, the values of the ligand protons were shifted to the down field in the ^{1}H-NMR spectrum.

The ligand's ^{13}C-NMR spectra revealed aromatic carbons in the range of 112.71–128.76 ppm and a 39.69 ppm (CH_3) group. Due to the coordination nature of the imine (-CH=N) group's participation in the formation of the metal complex, the imine CH=N carbon, which was previously detected in the ligand at 161.38 ppm, was shifted to the up field at 164.79 ppm. All other peaks [30] are relatively unchanged, as shown in **Figures 4a and b**.

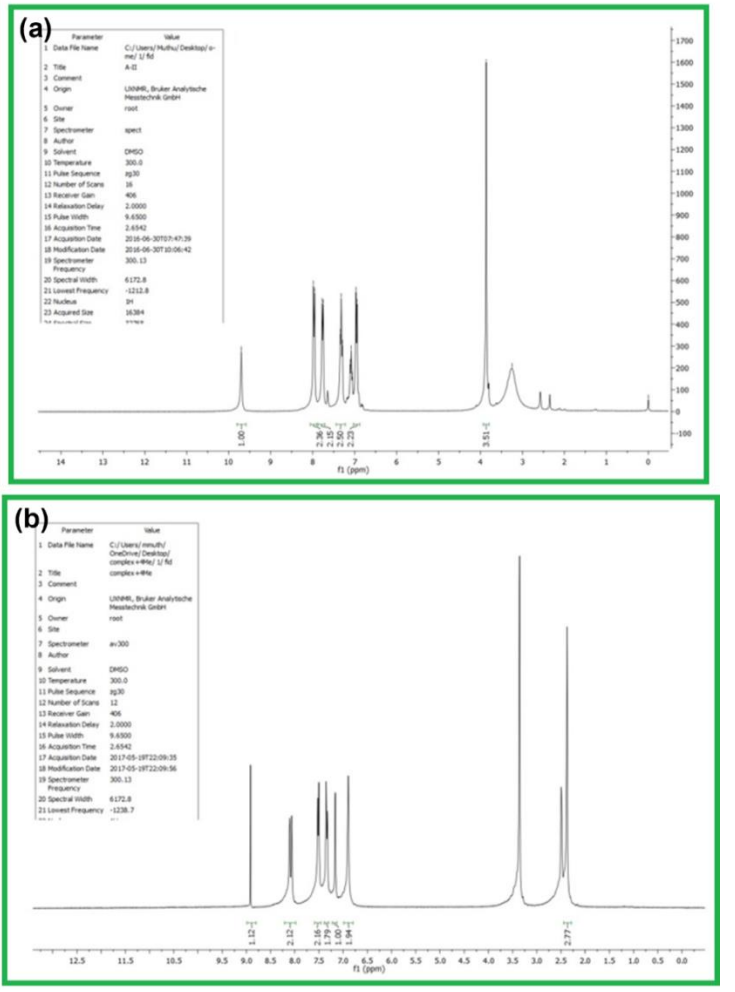

Figure 3. ^{1}H-NMR Spectra of **(a)** Ligand and **(b)**CuL_2 complex.

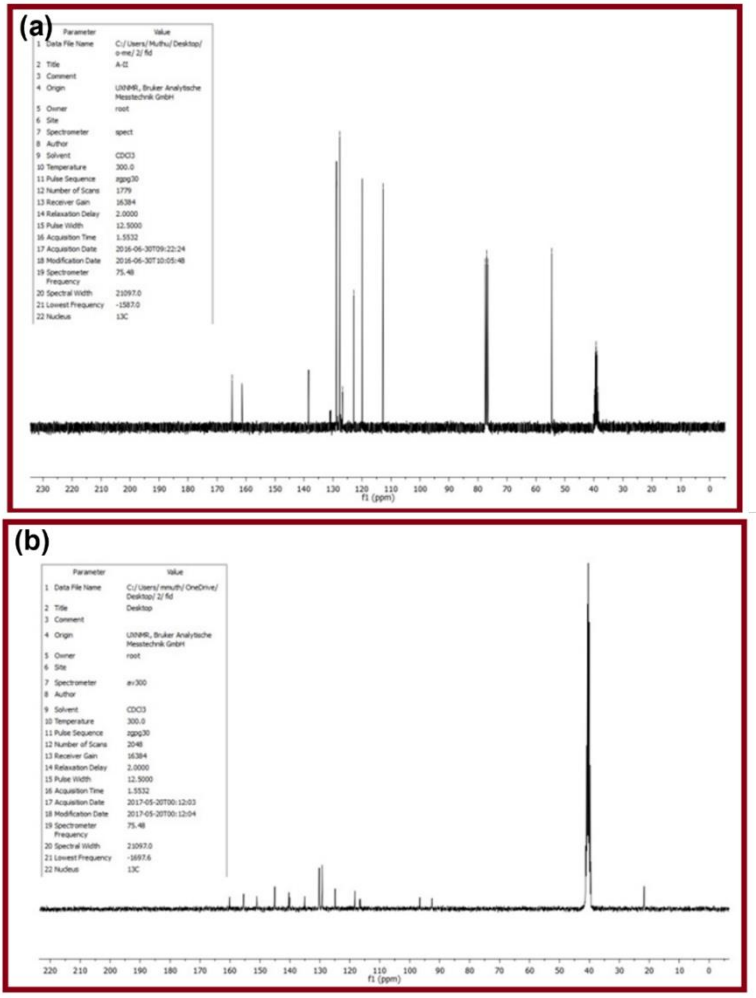

Figure 4. ^{13}C-NMR Spectra of **(a)** Ligand and **(b)**CuL_2 complex.

3.4 Mass Spectroscopy

The stoichiometric compositions of the ligand and chelates were confirmed by comparing the corresponding Mass spectra (**Figures 5a and 5b).** The observed molecular ion peak for the ligand (L) was 331 m/z, which supports the "Nitrogen rule" and shows the chelate contains four nitrogen. The molecular ion peak for copper complex was observed at 826 m/z, confirm the metal complexes were ML_2 stoichiometry. The mass spectra of other chelates also confirmed that their stoichiometry was the same [31]. The molecular ion (m/z) peaks

at 821, 822, and 828 correspond to the [CoL_2], [NiL_2], and [ZnL_2] complexes, respectively.

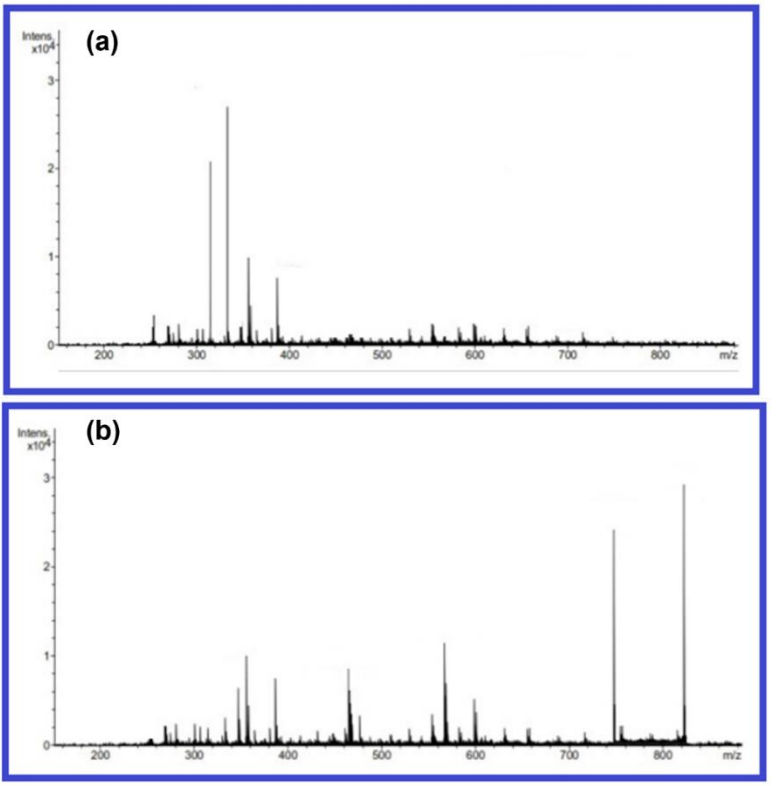

Figure 5. HR-Mass Spectra of **(a)** Ligand and **(b)** CuL_2 complex

3.5 Electron Paramagnetic Resonance Studies

The geometry and the nature of bond between the ligand and metal ions can both be examined using EPR spectroscopy. The Cu (II) complex's X-band EPR spectra (**Figure 6)** were captured at both RT and liquid N_2 temperature (LNT)[32]. In ESR of Cu (II) chelates, tumbling motion caused four peaks in lower region and one excessive peak in higher region. Due to molecules tumbling motion, isotropic excessive absorption was seen at higher region of spectra. **Table 3** shows the calculated spin Hamiltonian parameters for the Cu (II) complex. The calculated values $A_{||}(180) > A_{\perp}$ (93.4) of the axially symmetric g-tensor were $g_{||}$ (2.226) and $g_{\perp}$ (2.024). The higher

value demonstrating that Cu (II) complex in octahedral geometry [33-35]. Axes were seen to be in a tetragonal shape and the G value was found to be 4.70.

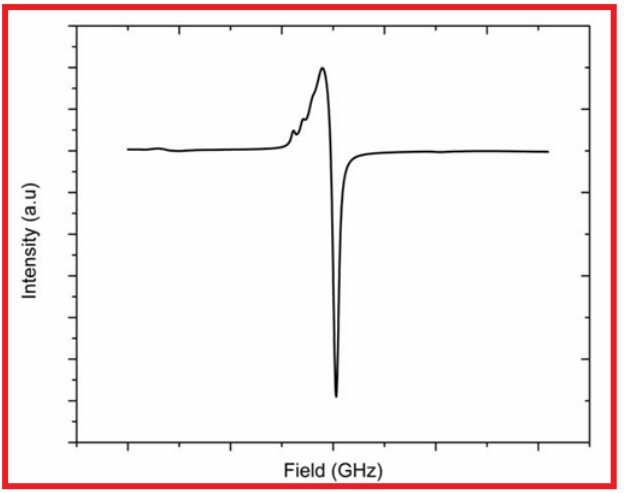

Figure 6. A EPR Spectrum of CuL_2 Complex.

Table 3. The DMSO solutions of CuL_2 complex's spin Hamiltonian parameters at LNT

Complex	g-tensor			A × 10^{-4} (cm^{-1})			$g_{\|\|}$/ $A_{\|\|}$	G
	$g_{\|\|}$	$g_{\perp}$	g_{iso}	$A_{\|\|}$	$A_{\perp}$	A_{iso}		
[CuL_2]	2.226	2.024	2.072	180	93.5	128.5	124	4.70

3.6. Fluorescence Spectroscopy (Emission Spectral Studies)

In fluorescence spectroscopy, the interactions of Ethidium bromide (EB) with DNA exhibits sensitive fluorescence for strongly binds [36]. The DNA along with EB does not fluoresce, but the intensity of its emission is greatly increased because of the strong intercalation with DNA base pairs. The intensity of fluorescence tells us how tightly the second molecule binds to the DNA [37]. **Figure 7** depicts the EB fluorescence intensity, which noticeably decreases as the complex concentration increases. The quenching plots demonstrate that the linear agreement between the Stern-Volmer relationship and the fluorescent quenching of EB bound to DNA by the synthesized chelates confirms the binding of two complexes. For the chelates of Zn(II), Ni(II), and Cu(II), the binding constants were 4.04 x 10^5 M^{-1}, 5.86 x 10^5 M^{-1}, and 6.82 x 10^5 M^{-1}, respectively.

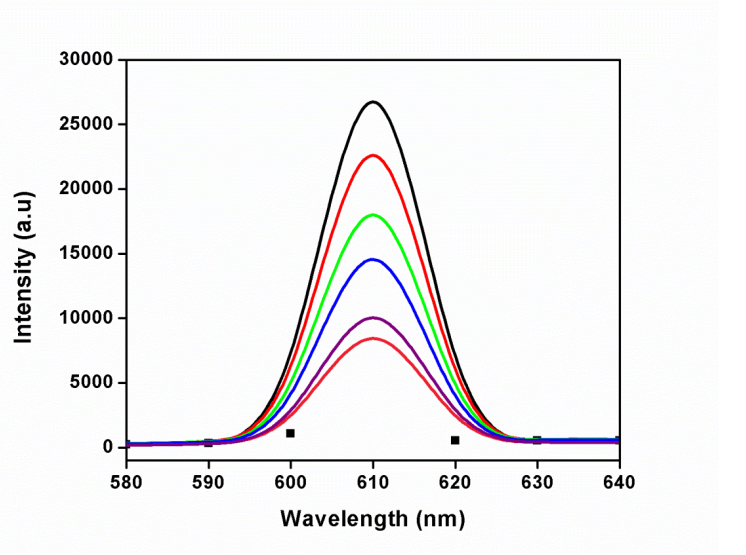

Figure 7. Fluorescence spectra of metal chelates bind with DNA

3.7. UV-Visible Absorption Studies

Electronic titration is one of the crucial techniques for examining the type of binding between CT DNA and metal complexes [38].

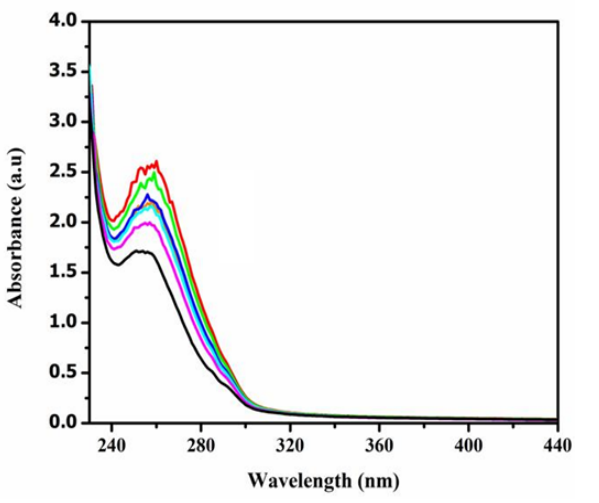

Figure 8. The [CuL_2] complex titration spectrum with increasing DNA concentration in buffer (pH = 7.2) at 25 °C.

Absorption spectra of metal chelates solution (10-3 M) were investigated with or without CT DNA (Figure 8). Upon adding the

30 ml of above solution to CT DNA, hyperchromic shift were seen. The π- π* transition in the range of 245-251 nm demonstrated the binding of CT DNA by all metal complexes. The hyperchromic bands show a groove-like mode of CT DNA and metal complex binding (39). Table 4 lists the calculated intrinsic binding constants (kb) for each metal complex. The order of the metal complexes binding efficiency was [Cu L]> [ZnL> [NiL] > [Co L]. In comparison to other metal complexes, the copper complex has a higher binding efficiency of 1.41 x 10-5 M kb.

Table 4. Absorption data for the prepared metal complexes interaction with CT DNA

Compound	**λ max(nm)**		**Δλ(nm)**	**[a]H%**	$k_b \times 10^5$ **(M^{-1})**
	Free	Bound			
[CuL]	256	256	5	1.9	2.41
[NiL]	248	252	4	1.6	1.75
[CoL]	251	255	4	1.5	1.35
[ZnL]	245	250	5	1.8	1.92

Note: [a]H% = $[(A_{free} - A_{bound}) / A_{free}] \times 100\%$

3.8 Measurements of Viscosity

Measurements of viscosity provided additional support for binding between the metal chelates with CT-DNA [40]. Figure 9 shows the viscosity measurements of metal complexes, EB with CT DNA at 30 ^oC. By varying the concentration of the metal chelates while maintaining a same CT DNA concentration, the viscosities of metal chelates were calculated. As more metal complexes were added, the relative DNA's viscosity gradually decreased. The bulky and steric nature of the metal complex causes the viscosity drops, when the metal chelates bound to CT DNA surface. These facts demonstrate that CT DNA and metal complexes bind to each other in a groove. When evaluating the other chelates, the copper chelate was more efficient at binding to CT DNA.

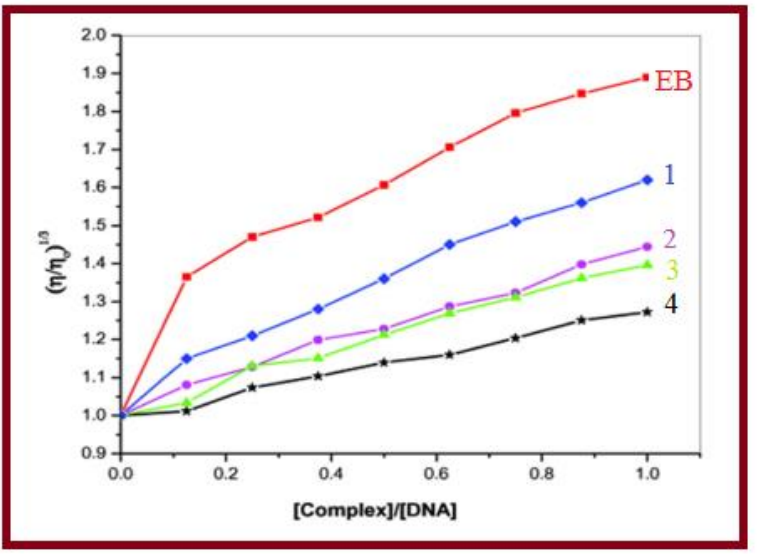

Figure 9. Measurement of viscosity of CT-DNA with increasing amounts of [EB] (♦), [CuL_2](1) (■), [NiL_2](2)(•),[CoL_2](3)(▲) and[ZnL_2](4)(∗)

3.9 In-Vitro Antimicrobial Studies

The zone inhibition of ligand and metal chelates against different bacterial strains were assessed using disc diffusion method. All the metal chelates were observed to be more reactive than the free ligands and the inhibitions were elucidated based on chelation theory and overtones concept [41]. Better activity against *Bacillus subtilis* and *Escherichia coli* has been demonstrated by the Cu (II) and Ni(II) complexes. The Co (II) complexes with *Bacillus subtilis* and *Escherichia coli* showed moderate activity. Although the ligands have demonstrated less activity against the bacterial stains *Bacillus subtilis* and *Escherichia coli*, the Zn (II) and Cu(II) complexes have moderate activity against *Bacillus subtilis*. The order of antibacterial activity was Cu>Zn>Ni>Co. The bacterial strains were treated with streptomycin as a standard medication [42]. **Figure 10** shows the antimicrobial activity of ligand and their complexes in *Escherichia coli* and *Bacillus subtilis*, and **Figure 11** displays the antimicrobial activity of as-synthesized metal complexes using various microbial strains.

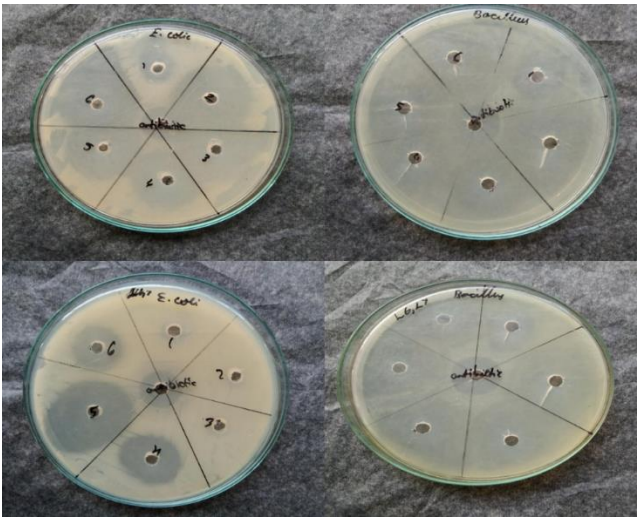

Figure 10. Zone inhibition of ligand and metal chelates against bacterial growth

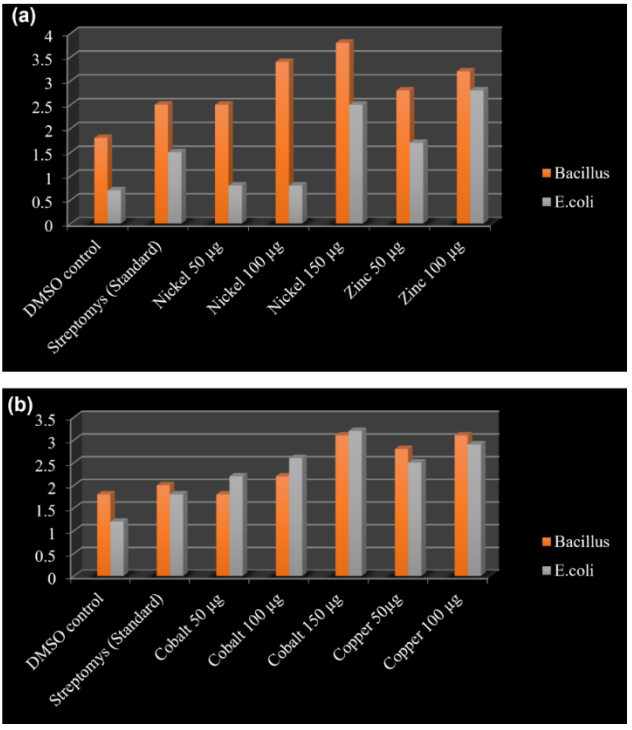

Figure 11. Antimicrobial properties of metal complexes in different microbial strains

4. Conclusion

Bidentate ligand (L) was prepared by Knoevenagel reaction between 4-bromobenzaldehyde and 2-amino-6-methylbenzothiazole. The synthesized metal Co(II), Ni(II), Cu(II), and Zn(II) chelates were characterized from corresponding spectra and physico-chemical techniques. UV spectral data confirmed the octahedral geometry of all of these chelates. Binding of the chelates with CT-DNA has been observed on fluorescence spectra and gel electrophoresis, and the results revealed that each chelate bound to DNA and cause fluorescence quenching. The in *vitro* antimicrobial effects of the chelates were examined against three fungi and four bacteria using the disc diffusion method. Metal chelates observed to have much higher MIC values rather than free ligand for inhibiting the growth of Bacteria.

References

1. Jeyamurugan R, Raman N, Synthesis, Characterization, Electrochemical Behaviour, DNA Binding and Cleavage Studies of Substituted β-Diketimine Copper(II) and Zinc(II) Complexes, IJIRSET. 4(2) (2015) 477- 485.
2. Dupureur C M, Barton J K, Structural Studies of Λ- and Δ-[Ru(phen)2dppz]2+ Bound to d(GTCGAC)2: Characterization of Enantioselective Intercalation. Inorg. Chem., 36 (1997) 33-43 .
3. Nair R B,Teng E S, Kirkland S L and Murphy C J, Synthes.is and DNA-Binding Properties of [Ru(NH(3))(4)dppz](2+). Inorg. Chem., 37 (1998) 139-141. L. Mishra, K. Bindu and L. C. Nathan, *Indian.J. chem*., **41A** (2002) 2533.
4. Nordan B, Lincoln P, Akerman B and Tuite E, In Metal Ions in Biological systems: Probing of Nucleic Acids by Metal Ion Complexes of Small Molecule, edited by A. Sigel and H. Sigel (Marcel Decker, Newyork), 33 (1996) 177.
5. Gellert M, et al., Cold Spring HarberSymps. Quant. Biol., 43 (1979) 35.

6. Foley F M ,Keene F R and Collins J G ,The DNA binding of the ΔΔ-, ΔΛ- and ΛΛ-stereoisomers of [{Ru(Me2bpy)2}2(μ-bpm)]4+ J.Chem. Soc. Dalton Trans, 21 (2001) 2968-2974.

7. Fitzgerald J A, Rauter H and Farrell N ,Approaches to Selective DNA Binding in Polyfunctional Dinuclear Platinum Chemistry. The Synthesis of a Trifunctional Compound and Its Interaction with the Mononucleotide 5′-Guanosine Monophosphate, Inorg. Chem., 40 (2001) 6324-6327.

8. Todd J A ,Rendina L M,Synthesis and DNA-Binding Properties of Cationic 2,2′:6′,2′ ′-Terpyridineplatinum(II) Complexes Containing 1,2- and 1,7-Dicarba-closo-dodecaborane Inorg. Chem.,41(2001) 3331-3333.

9. Zhang C X ,Lippard S J ,New metal complexes as potential therapeutics, Curr. Op. Chem. Biol., 7 (2003) 481-489.

10. Smith, J A. Collins, J G. Patterson B Tand Keene F R, Total enantioselectivity in the DNA binding of the dinuclear ruthenium(ii) complex [{Ru(Me2bpy)2}2(μ-bpm)]4+ {bpm = 2,2′-bipyrimidine; Me2bpy = 4,4′-dimethyl-2,2′-bipyridine},, J. Chem. Soc. Dalton Trans, 9 (2004) 1277-1283.

11. Sortino, S, Condorelli G, Complexes between fluoroquinolones and calf thymus DNA: binding mode and photochemical reactivity, New J. Chem., 26 (2002) 250-258.

12. Cusumano M , Di-Pietron M L, Giannetto A and Romano F, Influence of DNA on the Rate of Ligand Substitution in Platinum(II) Terpyridine Complexes, Inorg.Chem., 39 (2000) 50-55 .

13. Szacilowski K, Macyk W, Darzewiecka-Matuszek A, Brindell M and Stochel G,Bioinorganic Photochemistry: Frontiers and Mechanisms Chem. Rev., 105 (2005) 2647-2694 .

14. Alvarez M G, Alzuet G, Borras J , Macias B and Castineriras A, Oxidative Cleavage of DNA by a New Ferromagnetic Linear Trinuclear Copper(II) Complex in the Presence of H2O2/Sodium Ascorbate, Inorg. Chem., 42 (2003) 2992-2998.

15. Ren R, Yang P, Zheng W and Hua Z A ,Simple Copper(II)−l-Histidine System for Efficient Hydrolytic Cleavage of DNA. Inorg. Chem., 39 (2000) 5454-5463.

16. Reddy P A N, Nethaji M and Chakravarthy A R, Hydrolytic Cleavage of DNA by Ternary Amino Acid Schiff Base Copper(II) Complexes Having Planar Heterocyclic Ligands, Inorg. Chem., (2004) 1440-1446.

17. Raman N, Pravin N, DNA fastening and ripping actions of novel Knoevenagel condensed dicarboxylic acid complexes in antitumor journey, Eur. J. Med. Chem. 80 (2014) 57- 70.

18. Bosseggia E , Gatos M , Lucatello L , Mancin F , Moro S, Palumbo M , Sissi C, Tecilla P , Tonellato U and Zegotto G, Toward Efficient Zn(II)-Based Artificial Nucleases. Chem. Soc., 126 (2004) 4543-4549 .

19. Pathak R B, Thana B and Bahel S C, Antibacterial Antifungal agents, 8 (1980) 12.

20. Chohan Z H, Rauf A, Synth. React. Inorg. Met. Org. Chem., 26 (1996) 591.

21. Geary W, Geary W J. The Use of Conductivity Measurements in Organic Solvents for the Characterisation of Coordination Compounds. Coordination Chemistry. Chem.Rev.,7 (1971) 81-122.

22. Heim K E, Tagliaferro A R and Bobilya D J ,Nutr J, Flavonoid antioxidants: chemistry, metabolism and structure-activity relationships Biochem, 13 (2002) 572-584.

23. Bakir S R, Al-hamdani A A, and Jarad A, Synthesis and Characterization of Mixed Ligands of Dithizone and Schiff Base Complexes with Selected Metal Ions.Journal for Pure Sciences, 9 (2013) 82 -94.

24. Srivastava S D, Sen, J P, Synthesis and Biological Evaluation of 2- Amino benzo thiazole Derivatives.Indian Journal of Chemistry. 47B,10 (2008)1583-1586.

25. Speier G , Csihony J ,Whalen A M and Pierpont C G, Studies on Aerobic Reactions of Ammonia/3,5-Di-tert-butylcatechol

Schiff-Base Condensation Products with Copper, Copper(I), and Copper(II). Strong Copper(II)−Radical Ferromagnetic Exchange and Observations on a Unique N−N Coupling Reaction Inorg. Chem., 35 (1996) 3519-3524.

26. Sasma P K, Patra A K, Nethaji M , Chakravarty A R, DNA Cleavage by New Oxovanadium(IV) Complexes of N-Salicylidene α-Amino Acids and Phenanthroline Bases in the Photodynamic Therapy Window ., Inorg. Chem., 45 (2007) 11112-11121.

27. Abdel-Rahman L H, El-Khatib R M, Nassr, L A E, Abu-Dief A M, Lashin F E, Design, characterization, teratogenicity testing, antibacterial, antifungal and DNA interaction of few high spin Fe (II) Schiff base amino acid complexes, Spectrochim.Acta Part A. 111 (2013) 266 – 276.

28. Gaber M H, Ghamry A E, Fathalla S K, Mansour M A, Synthesis, spectroscopic, thermal and molecular modeling studies of Zn2 +, Cd2 + andUO22 + complexes of Schiff bases containing triazole moiety. Antimicrobial, anticancer,antioxidant and DNA binding studies, Mater. Sci. Eng. C. 83, 78-89.

29. Emara A A A, Spectrochim. Acta A. Structural, spectral and biological studies of binuclear tetradentate metal complexes of N3O Schiff base ligand synthesized from 4,6-diacetylresorcinol and diethylenetriamine 77 (2010) 117–125 .

30. Anna K. F. Mårtensson, Maria Abrahamsson, Eimer M. Tuite, Per Lincoln. Diastereomeric Crowding Effects in the Competitive DNA Intercalation of Ru(phenanthroline)2dipyridophenazine2+ Enantiomers. Inorganic Chemistry , 58 (14) (2019) , 9452-9459.

31. Vhanale B T , Deshmukh N J, Shinde A T, Synthesis, characterization, spectroscopic studies and biological evaluation of Schiff bases derived from 1–hydroxy-2-acetonapthanone, Heliyon, 5 (2019) e02774.

32. Utecht-Jarzyńska G, Michalak A, Banaś J, Mlostoń G, Jasiński M, Trapping of trifluoroacetonitrile imines with mercapto acetaldehyde and mercapto carboxylic acids: An

access to fluorinated 1,3,4-thiadiazine derivatives via (3+3)-annulation, J. Fluor. Chem.222–223 (2019) 8-14.

33. Freeman F , Properties and reactions of Ylidene malononitriles, Chem. Rev. 80 (1980) 329- 350.
34. Raman N, Joseph J, Sakthivel A, Jeyamurugan R, Synthesis, structural, characterization and antimicrobial studies of novel schiff base Copper(II) Complexes, J. Chil. Chem. Soc. 54 (4) (2009) 354-357.
35. Ramesh R, Maheshwaran S, Synthesis, spectra, dioxygen affinity and antifungal activity of Ru(III)Schiff base complexes, J. Inorg. Biochem. 96 (2003) 457-462.
36. Al – Mohammed N. N, Alias Y, Abdullah Z, Shakir R M, Taha E M, Hamid A A, Synthesis and antibacterial evaluation of some novel imidazole and benzimidazole sulfonamides, Molecules, 26 (2013) 11978- 11995.
37. Shukla S N, Gaur P, Lal Raidas M , Chaurasia B, Tailored synthesis of unsymmetrical tetradentate ONNO schiff base complexes of Fe(III), Co(II) and Ni(II): Spectroscopic characterization, DFT optimization, oxygenbinding study, antibacterial and anticorrosion activity, J. Mol. Stru. 1202 (2020) 127362- 127371.
38. Saddam Hossain M D, Zahid A A S M, Zakaria C M, Anti-pathogenic Activity of Cu(II) Complexes Incorporating Schiff Bases,American Journal of Heterocyclic Chem5(1)(2019) 11-23.
39. Raman N, Mahalakshmi R , Bio active mixed ligand complexes of Cu(II), Ni(II) and Zn(II): Synthesis, spectral, XRD, DNA binding and cleavage properties, Inorganic Chemistry Communications 40 (2014) 157–163.
40. Hossain S , Camellia F K, Uddin N , Banu L A and Haque M , Synthesis, Characterization and Antimicrobial Activity of Metal Complexes of N-(4-methoxybenzylidene) Isonicotinohydrazone Schiff Base, 6 (2019) 1-8 .
41. Tyagi P , Tyag M, Agrawal S , Chandra S, Ojha H, Pathak M , Synthesis, characterization of 1,2,4-triazole Schiff base

derived 3d-metal complexes: Induces cytotoxicity in HepG2, MCF-7 cell line, BSA binding fluorescence and DFT study.

42. Tyagi P, Chandra S, Saraswat B S, Ni(II) and Zn(II) complexes of 2-((thiophen-2-ylmethylene)amino) benzamide: Synthesis, spectroscopic characterization, thermal, DFT and anticancer activities, Biomolecular Spectroscopy 134 (2015) 200–209.